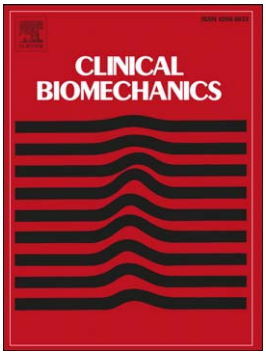

Femoral Shaft Strains During Daily Activities: Implications For Atypical Femoral Fractures

Saulo Martelli, Peter Pivonka, Peter R. Ebeling

PII: S0268-0033(14)00191-0
DOI: doi: 10.1016/j.clinbiomech.2014.08.001
Reference: JCLB 3824

To appear in: *Clinical Biomechanics*

Received date: 18 March 2014
Revised date: 23 June 2014
Accepted date: 4 August 2014

Please cite this article as: Martelli, Saulo, Pivonka, Peter, Ebeling, Peter R., Femoral Shaft Strains During Daily Activities: Implications For Atypical Femoral Fractures, *Clinical Biomechanics* (2014), doi: 10.1016/j.clinbiomech.2014.08.001

FEMORAL SHAFT STRAINS DURING DAILY ACTIVITIES: IMPLICATIONS FOR ATYPICAL FEMORAL FRACTURES

Saulo Martelli[1,2], Peter Pivonka[2,3], Peter R. Ebeling[2,3]

1 Medical Device Research Institute, School of Computer Science, Engineering and Mathematics, Flinders University, Adelaide SA, Australia

2 North West Academic Centre, The University of Melbourne, St Albans, Australia

3 Australian Institute for Musculoskeletal Science, St Albans, Australia

Submitted as an original full-length article to Clinical Biomechanics

Word count (Introduction to Discussion): 3925/4000. Word count (Abstract): 249/ 250

Figures count: 6, Tables count: 1. Supplementary material: 7 figures

Corresponding author:

Saulo Martelli, Ph.D.

Medical Device Research Institute

School of Computer Science, Engineering and Mathematics

Flinders University

South Australia 5000, Australia

Phone: +61 8 82012674

E-mail: saulo.martelli@flinders.edu.au

ABSTRACT

Background

Atypical femoral fractures are low-energy fractures initiating in the lateral femoral shaft. We hypothesized that atypical femoral fracture onset is associated with daily femoral strain patterns. We examined femoral shaft strains during daily activities.

Methods

We analyzed earlier calculations of femoral strain during walking, sitting and rising from a chair, stair ascent, stair descent, stepping up, and squatting based on anatomically consistent musculoskeletal and finite-element models from a single donor and motion recordings from a body-matched volunteer. Femoral strains in the femoral shaft were extracted for the different activities and compared. The dependency between femoral strains in the lateral shaft and kinetic parameters was studied using multi-parametric linear regression analysis.

Findings

Tensile strain in the lateral femoral shaft varied from 327 με (squatting) to 2004 με (walking). Walking and stair descent imposed tensile loading on the lateral shaft, whereas the other activities mainly imposed tensile loads on the anterior shaft. The multi-parametric linear regression showed a moderately strong correlation between tensile strains in the lateral shaft and the motion kinetic (joint moments and ground reaction force) in the proximal (R^2 = 0.60) and the distal shaft (R^2 = 0.46).

Interpretation

Bone regions subjected to tensile strains are associated with atypical femoral fractures. Walking is the daily activity that induces the highest tensile strain in the lateral femoral shaft. The kinetics of motion explains 46%-50% of the tensile strain variation in the lateral shaft, whereas the unexplained part is likely to be attributed to the way joint moments are decomposed into muscle forces.

Keywords: Atypical femoral fracture; femoral strain patterns; physical activity; musculoskeletal and finite-element modeling; osteoporosis; anti-resorptive therapy

1. Introduction

Atypical femoral fractures (AFFs) are rare low-energy stress fractures progressing from the lateral femoral shaft to complete predominantly transverse fractures (Shane et al., 2010). Approximately 25% of AFF patients die within two years, while most survivors experience permanent disabilities (Ekström et al., 2009). The increasing interest of the research community (Shane et al., 2013, 2010) in these rare femoral fractures is to be attributed to the suspected role played in AFFs by anti-resorptive therapies, most commonly and increasingly used to treat patients with osteoporosis (Dell et al., 2010). Indeed, long-term (i.e., ~ 3 years and above) anti-resorptive therapy may affect bone repair and its mechanical properties increasing bone's susceptibility to stress fractures (Allen et al., 2008; Benhamou, 2007). However, the systemic bone changes caused by anti-resorptive drugs cannot explain the specific location where AFFs onset takes place. A complementary explanation for AFFs may reside in the daily mechanical environment of the femoral shaft.

AFFs resemble stress fractures and pseudo-fractures of the femoral shaft and occur anywhere from just below the lesser trochanter to the distal femoral metaphysis (Shane et al., 2013). AFFs are often preceded by prodromal pain with formation of a callus in the lateral cortex adjacent to the fracture onset, are associated with absence or low trauma, are not comminuted and are mainly transverse in orientation. Investigations into the effect of long-term anti-resorptive therapy on the bone mechanical properties showed different and at times contrasting effects, either promoting or reducing the collagen matrix toughness (Vashishth, 2009); increasing bone mineralization; leveling the mineral particles shape and orientation, and narrowing the bone mineralization density distribution (BMDD) (Bala et al., 2012; Boivin et al., 2000; Roschger et al., 2001); and suppressing excessive bone remodeling causing a bone strength increase (Li et al., 2001) while, at the same time, facilitating microdamage accumulation (Allen and Burr, 2007). While anti-resorptive therapy may

increase bone fragility, creating conditions conducive to development of AFFs, the drug's systemic and generalized effect on the femur tissue does not justify the localized and recurrent AFFs onset in a specific femoral region, that is, the lateral shaft. One possible explanation is that the femoral shaft is subjected to daily loads that, eventually combined with altered bone mechanical properties, create the most favorable environment for AFFs in the lateral region. Two alternative theories have commonly been applied to describe daily femoral shaft loads (Aamodt et al., 1997). The classic Pauwels' theory states that the femur is subjected to a frontal-plane bending moment generated by the gluteals and the tractus iliotibialis, causing tension on the lateral and compression on the medial femur (Kummer, 1993), whereas Fetto and Austin (1994) theorized that muscular forces lead to a moment-free loading, causing a uniform compressive state throughout the femoral shaft. Both theories, however, are based on a simple static unilateral stance activity. The experimental evidence supporting either theory is limited. The increased risk for AFFs in subjects with tibio-femoral misalignment (Saita et al., 2012) and pronounced femoral bowing (Sasaki et al., 2012) have been attributed to an increased femoral bending, causing tension in the lateral femoral shaft. Aamodt et al. (1997) reported tensile strains directly measured in a single location of the lateral femoral shaft for two patients. Theoretical investigations reported femoral strain patterns characterized by combined bending and torsion on a synthetic femur, mimicking walking (Duda et al., 1998). However, no studies have reported 3D tensile and compressive strain distributions in the femoral shaft during different daily activities. It possible that typical strain patterns in the femoral shaft are activity type-dependent and that some of them create a more favorable condition for AFFs in the lateral cortex. In this study, we focus on typical strain patterns in the femoral shaft during activities of daily living.

The only viable way to estimate 3D in-vivo femoral strain distributions is through computational modeling. Musculoskeletal models can be used to calculate muscle and joint

forces (Delp et al., 2007; Martelli et al., 2011) that serve as boundary conditions of finite-element (FE) models for the calculation of the bone strain distribution (Keyak et al., 1993; Schileo et al., 2007). A few years ago, the EU-funded project Living Human Digital Library (LHDL, IST-2004-026932) made publicly available a complete data collection from a healthy 81 year old female donor (www.physiomespace.com), which included the full body dissection, clinical computed-tomography (CT), magnetic resonance images (MRI), and experimental measurements of femoral strains. This data were used to generate and validate a finite-element model of the femur and the musculoskeletal model of the donor's lower-limb, resulting in a unique consistency of models in either topological or geometrical terms. The femur finite-element model was shown to predict well experimental measurements of bone strains taken on the same bone under multi-axial loads ($R^2 = 0.95$) while the musculoskeletal model yielded calculations of the hip contact force in agreement with corresponding measurements taken from THR patients between 51 and 76 years of age (Martelli et al., 2014). Therefore, these models can be used to study the typical patterns of physiological strains in the femoral shaft of elderly women.

The aim of this study was to test the hypothesis that the predicted location of AFF onset is associated with the patterns of femoral strain during daily activities. Moreover, we tested the hypothesis that bone strains in the lateral femoral shaft are determined by the hip abduction moment according to Pauwels' theory. To these aims, we analyzed earlier simulations of femoral strains obtained using the aforementioned models (Martelli et al., 2014) by focusing on the femoral shaft.

1. Materials and methods

Cortical strains in the femoral shaft were studied by combining experimental motion data and models of femoral elasticity and forces (Figure 1). Models and simulations were developed and run during an earlier study where further details can be found (Martelli et al., 2014). In the present study, tensile and compressive strains in the femoral shaft were collected and analyzed; motion data and models are described below with the sole intent of providing the reader with a clear context for analysis. Models comprised a musculoskeletal model of the lower limb and a femur finite-element model from a single donor to ensure that no bias in the results was made by the topological and geometrical differences between the two models.

2.1 Physical activities

The body-matched volunteer (female, 25 years old) was selected by measuring anthropometry and body weight to match that of the donor's (Table 1). Body height and weight were measured using a commercial meter and scale. The pelvis width was assumed the distance between the right and left anterior superior iliac spine (ASIS), the femoral length was assumed the distance between the ASIS and the lateral femoral epicondyle (LE), and the shank length was assumed the distance between LE and the lateral tibial malleolus (LM). Individual measurements were taken thrice, and then, averaged.

The participant was equipped with 51 skin-mounted reflective markers (10 mm. in diameter) positioned according to the protocol proposed by Leardini et al. (2007). Motion data comprised the marker trajectories and the ground reaction force (GRF) collected during five repetitions of stair ascent (32 cm. high, 54 cm. step depth), stair descent, rising from and lowering into a chair (42.5 cm. high), step up (17 cm. high), and squatting and walking at a self-selected speed (1.2 m·s-1). Marker trajectories were collected using an eight-camera motion system (Vicon Motion Capture, Oxford UK), using a sampling rate of 100 Hz. GRF

data were recorded using two force platforms (Kistler Instrument AG, Switzerland), using a sampling rate of 2000 Hz. Ground reaction force patterns displayed consistency with corresponding normality patterns (Bergmann et al., 2001; Stacoff et al., 2005) (Supplemental figure 1).

2.2 Musculoskeletal model

The donor's lower-limb musculoskeletal model was used to calculate the muscle and joint reaction forces acting on the femur during the investigated activities. All simulations were performed using an open-source musculoskeletal modeling environment called OpenSim (Delp et al., 2007). The body was modeled as a 13-segment, 15 degree-of-freedom (DOF) articulated system, actuated by 84 muscle-tendon units. The skeletal anatomy was extracted from the donor's full-body CT scan. Inertial properties of each segment were derived from the CT images, assuming homogeneous density properties for both the hard (1.42 g/cm^3) and soft (1.03 g/cm^3) tissues (Dumas et al., 2005). The lower-limb muscle system was defined by registering a generic model (Delp et al., 1990) on the donor's anatomy using anatomy texts (Clemente, 1985) and dissection data (Valente et al., 2012) as references. The muscles' peak isometric force was calculated using the physiological cross-sectional areas extracted from the MRI images and a specific muscle tension of 1 MPa (Glitsch and Baumann, 1997). The position of the virtual markers reported by Leardini et al. (2007) was identified in the musculoskeletal model using the donor's skin surface extracted from the CT images. No scaling of the musculoskeletal model was necessary to adjust the model to the body-matched anatomy of the volunteer because the volunteer and the donor were body-matched, resulting in similar intra-segmental lengths at the pelvis, thigh, and shank, and had similar body weight and height (Table 1).

The joint angle trajectories were calculated by minimizing the instantaneous sum of the squared distances between the volunteer's skin-mounted markers and the virtual markers

in the model. The net joint moments were calculated using inverse dynamics from the joint angle trajectories and the measured GRF. A static optimization problem was solved to decompose the net joint moments amongst the muscles by minimizing the weighted squared sum of muscle activations (Heintz and Gutierrez-Farewik, 2007). The hip contact force was calculated by solving for the static equilibrium at the femur.

The model yielded joint angles, moments, and muscle firing patterns in agreement with normality patterns published for normal walking and hip reaction forces and in agreement with the envelope of corresponding measurements taken from THR patients between 51 and 76 years of age (Bergmann et al., 2001), during walking, stair ascent, stair descent, and rising from and sitting on a chair (Supplemental figures 2 and 3).

2.3 Finite-element model

The bone geometry was segmented from the CT images (pixel size: 0.5 mm) using medical image processing software (Amira©, Visage Imaging GmbH, USA). Bone tissue was modeled using 10-node tetrahedral elements of a mean element length of 2 mm. The bone apparent density distribution was extracted from the CT images by calibrating the image grey levels (Schileo et al., 2007). The femur was classified osteoporotic (T-score =-2.5) by extracting the femoral neck T-score from the CT images (Kröger et al., 1999). The Young's modulus distribution was calculated from the bone apparent density distribution using the relationship found by Morgan et al. (2003). A Poisson's ratio of 0.3 was assumed (Schileo et al., 2007). The mesh element's isotropic Young's modulus was calculated by integrating the image's voxel-based Young modulus over the mesh elements volume using Bonemat© (Super Computing Solutions, Italy). The model was kinematically fully constrained at the femoral epicondyles. Correlation between calculated and measured principal tensile and compressive strain was R^2 = 0.95, the Root Mean Square Error was 12.5% and the slope of the linear regression equation was 1.15 (Martelli et al., 2014).

Femoral shaft strains during different physical activities were calculated by applying the muscle and hip joint reaction forces to the femur finite-element model using an in-house Matlab (The MathWorks Inc., USA) routine. The topological and geometrical consistency between the musculoskeletal model and the femur model ensured that the equilibrium of forces was not disturbed. The local coordinate system of the right femur finite-element model and those of the pelvis, right femur, and right tibia in the musculoskeletal model were defined according to the International Society of Biomechanics (ISB) standards (Wu et al., 2002) and tracked during every studied activity. The muscle attachment and via points in the pelvic and tibial segments were read into the femur coordinate system. The muscle force unit vector was calculated using the femoral attachment point and its closest neighborhood along the muscle line of action. The muscle force vector was calculated by multiplying the muscle unit vector and the available force magnitude and applied to the femoral mesh closest node to the muscle attachment point in the musculoskeletal model. The hip joint was assumed frictionless. The hip load was applied on the femoral head surface, on the closest node to the hip force direction passing through the hip centre (Supplemental figures 4). Simulations were performed in Abaqus© (Dassault Systemes, USA) using the available direct solver. Fifteen time intervals uniformly distributed within the stance phase of each activity were simulated, resulting in a total of 90 linear-elastic simulations.

Principal tensile and compressive strain field were evaluated at four transversal section uniformly distributed between the subcapital region and the distal diaphysis (level A, B, C, and D). On each section, strain values were collected on the bone surface at 45° intervals, assuming 0° on the anterior femur and positive medial rotations. All the strain measurements were obtained by averaging the nodal strain results within 4 mm distance from the location being assessed. Continuous strain patterns were interpolated. The strain levels reached during the different activities were compared by calculating the principal tensile and

compressive strains along the frontal, posterior, medial, and lateral femoral shaft. Ten uniformly distributed locations between the subcapital region and the distal epiphysis were evaluated for each femoral aspect. For each of the ten locations and the four femoral aspects, principal tensile and compressive strain were averaged over the stance phase of each activity. Linear regression analysis was conducted to expose dependencies between cortical strain in the lateral femoral shaft and moments acting on the femur to test Pauwels' theory during different activities.

2. Results

The lateral aspect of the femur was subjected to tensile strains during all the investigated activities. Figure 2 shows the association between typical locations for AFFs as reported by Saleh et al. (2012) and tensile strains in the femoral shaft while walking. Both strain intensity and orientation in the transverse plane was activity-dependent, with walking showing the highest average tensile strains in correspondence with the location of onset of commonly observed AFFs.

The lateral femoral shaft (270°-300° in the transverse plane) was subjected to peak tensile loads during most of the walking stance phase, whereas the peak tensile strain was slightly rotated anteriorly during stair descent (270°-330°). The neutral plane was mainly sagittal, and the peak compressive strain was mainly located in the medial femoral shaft (0°-180° in the transversal plane). The anterior femoral shaft (315°-45° degrees in the transverse plane) was subjected to peak tensile loads during most of the chair up-and-down, squatting, stair ascent, and step-up stance phases. The neutral plane was mainly coronal, and the peak compressive strain was mainly located in the posterior femoral shaft (0°-180° in the transversal plane). The strain field in the transverse plane rotated from maximal tension in the proximal-lateral shaft to maximal tension in the distal-anterior shaft during the mid-stance phase of stair ascent indicating torsion. Figure 3 and 4 represent tensile and compressive

strain paths on transversal shaft sections during walking and stair ascent, which showed extreme strain field orientations. Strain patterns for stepping up, rising from and sitting on a chair, squatting, and stair descent are reported in the Supplementary Material.

The strain levels varied between activities. In the lateral femoral shaft, the average tensile strain during the stance phase of each activity varied from 327 με while squatting to 2004 με while walking, and from 245 με while squatting to 2337 με during stair rising in the anterior femoral shaft. In the medial femoral shaft, the average compressive strain varied from -369 με during stair ascent to -1942 με while walking, while it varied from -305 με while squatting to -2560 με during stair ascent in the posterior femoral shaft (Figure 5).

Tensile strain in the proximal-lateral femoral shaft (level A) was correlated with the hip abduction moment; the coefficient of determination was $R^2 = 0.94$ (p-value < 0.0001) during walking and $R^2 = 0.96$ (p-value < 0.0001) during stair ascent (Figure 6). In the distal-lateral femoral shaft (level D), the coefficient of determination was $R^2 = 0.50$ while walking and $R^2 = 0.09$ during stair ascent. No correlation was found between tensile strain and the hip abduction moment during the remaining activities. The multi-parametric linear regression analysis using the hip, knee, ankle moment and the ground reaction force intensity as predictors of tensile strains in the lateral femoral shaft during all the studied activities showed a moderately strong correlation in the proximal ($R^2 = 0.60$, p-value < 0.0001) and in the distal femoral shaft ($R^2 = 0.46$, p-value < 0.0001).

3. Discussion

Atypical femoral fractures (AFFs) are typically transverse stress fractures arising in the lateral femoral shaft (Shane et al., 2013). While AFFs have been associated with increased bone fragility and long-term anti-resorptive therapy (Shane et al., 2013), it is largely unknown why these fractures propagate from the lateral femoral shaft. We tested the

hypothesis that the location of AFFs onset is associated with physiological strain distribution during daily activities and that the tensile loads in the lateral femoral shaft are to be attributed to the hip abduction moment. We compared calculated femoral tensile strain distribution during walking, stair ascent, stair descent, standing from and sitting on a chair, step up, and squatting with common locations of AFFs onset.

The lateral femoral shaft is subjected to tensile strains during a variety of physical activities and walking induces the highest tensile strain levels. The hip abduction moment well predicts tensile strains in the lateral femoral shaft during walking and stair ascent, but not during a generic activity. The lateral aspect of the femoral shaft was loaded in tension during every studied activity. Therefore, the combination of tensile loads, to which bone is most susceptible (Bayraktar et al., 2004), and increased bone fragility that may be associated with long-term anti-resorptive therapy (Shane et al., 2013) may be an important co-factor in creating a favorable environment for AFFs. Tensile strain magnitudes and orientation in the transverse plane were activity-dependent, with walking inducing most of the tension in the lateral femoral shaft, whereas chair up-and-down, squatting, stair ascent, and step-up induced tension in the anterior femoral shaft. Walking is likely the most critical activity in individuals susceptible to AFFs, inducing high tensile strain in the lateral femoral shaft, most frequently during normal living. A reduced walking speed may help reduce tensile strains in the lateral femoral shaft by causing a reduction of the muscle work (Neptune et al., 2008) and of the ground reaction force (Nilsson and Thorstensson, 1989).

The hip abduction moment was strongly correlated with tensile strains in the proximo-lateral femoral shaft (levels A and B) during walking and stair ascent (Figure 6), in agreement with the classical Pauwels' theory (Kummer, 1993). However, we found no correlation between tensile strains in the lateral femoral shaft and the hip abduction moment during a generic activity (figure 6), whereas the multi-parametric linear regression showed that

multiple kinetic variables (i.e., the hip, knee, and ankle moments and the ground reaction force intensity) are predictors of tensile strains in the proximo-lateral (R^2 = 0.6) and the distal-lateral (R^2 = 0.46). This means that46-60% of the tensile strain variance in the lateral femoral shaft can be explained by the whole body dynamics, whereas the unexplained part (i.e. 40-54% of the strain variance) is likely to be attributed to other factors, such as musculoskeletal architecture and muscle recruitment strategy, influencing the process of decomposing the joint moments into muscle and joint forces. A deeper understanding of relationship between the body dynamics and femoral strain patterns would expose the mechanisms driving fractures, including low-energy stress fractures like AFFs.

Our results are consistent with earlier studies of bone strains (Aamodt et al., 1997; Biewener, 1990; Duda et al., 1998). Strain measurements (Aamodt et al., 1997) from a single location in the lateral-proximal femoral shaft for two "snapping hip syndrome" patients showed dominant tensile conditions during walking, stair ascent and one legged stance in agreement with present findings. The calculated strain range (0-4667 με) is consistent with the bone strain levels reported for mammalian bones during daily activities (25-50% of the yield strain) (Biewener, 1990). Earlier computational simulations of a synthetic femur (Duda et al., 1998) yielded up to 2000 με during walking, in good agreement with our results obtained for the initial two-third of the walking stance whereas our calculations of tensile strains during early heel rise were higher (4667 με). This discrepancy is likely caused by the single circumstance where the ground reaction force recorded from the volunteer (1.33BW) overestimated by ~30% corresponding normality patterns (Bergmann et al., 2001; Stacoff et al., 2005) (Supplemental figure 1). For the remaining walking phases and activities, kinetic variables and hip forces were in good agreement with corresponding measurements taken from THR patients between 51 and 76 years of age (Bergmann et al., 2001; Stacoff et al., 2005) (Supplements figure 3) providing good confidence on the present results.

Our study has some limitations. First, muscle and joint forces from a young volunteer may differ from those present in older adults. However, this appears not to be true for the motion data used in the present study because the calculated hip-joint reaction force, which includes the contributions of all the hip-spanning muscles, was consistent with published measurements (Bergmann et al. 2001) in older adults. This observation is consistent with the work of Lim et al. (2012) that showed no significant differences in lower-limb muscle forces when younger and older adults walk at the same speed. Second, results were generated using one anatomical dataset. It is possible that the inclusion of additional subjects may lead to different levels of bone strain in the femoral shaft. Further population-based studies are necessary to investigate how individual anatomical parameters, bone quality, and motion patterns affect the calculated strain patterns. Multi-scale computational modeling combining musculoskeletal and finite-element models are well suited to provide such important information. Third, the untreated osteoporotic donor's femur did not account for the contrasting 9.6% BMD increase after 3 years (Boivin et al., 2000) and 12% young modulus decrease after 6-10 years (Bala et al., 2012) of anti-resorptive therapy. Therefore, conclusions of the present study are directly relevant to persons who do not use anti-resorptive therapy. In the author's opinion, however, the validity of our study lies in the fact that it provides new insights into our understanding of the typical patterns of femoral loads applied to common sites of origin of AFFs and of the mechanical environment associated with AFF onset, i.e., tensile strain, and its changes during daily activities. Last, the association between tensile loads and AFF onset location shown here does not imply a cause-effect relationship between tensile strain and the pathogenesis of AFFs. Present results can provide a new base for designing new experiments investigating the mechanism of AFFs.

4. Conclusion

AFFs are associated with tensile strain conditions during each daily activity, with walking causing the highest tensile strain in the lateral femur. Therefore, tensile conditions are the most likely mechanical environment contributing to AFF onset. The hip abduction moment is the major determinant of tensile strain in the proximal-lateral femoral shaft during walking and stair ascent. However, this is not valid for a generic activity for which a more complex interaction between dynamic parameters, muscle architecture and recruitment strategy determines the tensile strain in the lateral femoral shaft.

ACKNOWLEDGMENTS

The authors are grateful to the EU-funded project LHDL (IST- 2004-026932) for the data made available. This study was supported by the Australian Research Council (DE140101530) awarded to S.M.

REFERENCES

Aamodt, A., Lund-Larsen, J., Eine, J., Andersen, E., Benum, P., Husby, O.S., 1997. In vivo measurements show tensile axial strain in the proximal lateral aspect of the human femur. J. Orthop. Res. 15, 927–31. doi:10.1002/jor.1100150620

Allen, M.R., Burr, D.B., 2007. Three years of alendronate treatment results in similar levels of vertebral microdamage as after one year of treatment. J. Bone Miner. Res. 22, 1759–65. doi:10.1359/jbmr.070720

Allen, M.R., Gineyts, E., Leeming, D.J., Burr, D.B., Delmas, P.D., 2008. Bisphosphonates alter trabecular bone collagen cross-linking and isomerization in beagle dog vertebra. Osteoporos. Int. 19, 329–37. doi:10.1007/s00198-007-0533-7

Bala, Y., Depalle, B., Farlay, D., Douillard, T., Meille, S., Follet, H., Chapurlat, R., Chevalier, J., Boivin, G., 2012. Bone micromechanical properties are compromised during long-term alendronate therapy independently of mineralization. J. Bone Miner. Res. 27, 825–34. doi:10.1002/jbmr.1501

Bayraktar, H.H., Morgan, E.F., Niebur, G.L., Morris, G.E., Wong, E.K., Keaveny, T.M., 2004. Comparison of the elastic and yield properties of human femoral trabecular and cortical bone tissue. J. Biomech. 37, 27–35. doi:10.1016/S0021-9290(03)00257-4

Benhamou, C.-L., 2007. Effects of osteoporosis medications on bone quality. Joint. Bone. Spine 74, 39–47. doi:10.1016/j.jbspin.2006.06.004

Bergmann, G., Deuretzbacher, G., Heller, M., Graichen, F., Rohlmann, A., Strauss, J., Duda, G.N., 2001. Hip contact forces and gait patterns from routine activities. J. Biomech. 34, 859–871.

Biewener, a a, 1990. Biomechanics of mammalian terrestrial locomotion. Science 250, 1097–103.

Boivin, G.Y., Chavassieux, P.M., Santora, A.C., Yates, J., Meunier, P.J., 2000. Alendronate increases bone strength by increasing the mean degree of mineralization of bone tissue in osteoporotic women. Bone 27, 687–94.

Clemente, C., 1985. Gray's Anatomy of the Human Body (30th Edition). Lea & Febiger.

Dell, R., Denise, G., Ott, S., Silverman, S., Eisemon, E., Funahashi, T., Adams, A., 2010. A Retrospective Analysis of all Atypical Femur Fractures Seen in a Large California HMO from the Years 2007 to 2009, in: ASBMR 2010 Annual Meeting. Toronto.

Delp, S.L., Anderson, F.C., Arnold, A.S., Loan, P., Habib, A., John, C.T., Guendelman, E., Thelen, D.G., 2007. OpenSim: open-source software to create and analyze dynamic simulations of movement. IEEE Trans. Biomed. Eng. 54, 1940–1950.

Delp, S.L., Loan, J.P., Hoy, M.G., Zajac, F.E., Topp, E.L., Rosen, J.M., 1990. An interactive graphics-based model of the lower extremity to study orthopaedic surgical procedures. IEEE Trans. Biomed. Eng. 37, 757–767.

Duda, G.N., Heller, M., Albinger, J., Schulz, O., Schneider, E., Claes, L., 1998. Influence of muscle forces on femoral strain distribution. J. Biomech. 31, 841–6.

Dumas, R., Aissaoui, R., Mitton, D., Skalli, W., de Guise, J. a, 2005. Personalized body segment parameters from biplanar low-dose radiography. IEEE Trans. Biomed. Eng. 52, 1756–63. doi:10.1109/TBME.2005.855711

Ekström, W., Németh, G., Samnegård, E., Dalen, N., Tidermark, J., 2009. Quality of life after a subtrochanteric fracture: a prospective cohort study on 87 elderly patients. Injury 40, 371–6. doi:10.1016/j.injury.2008.09.010

Fetto, J.F., Austin, K.S., 1994. A missing link in the evolution of THR: "discovery" of the lateral femur. Orthopedics 17, 347–51.

Glitsch, U., Baumann, W., 1997. The three-dimensional determination of internal loads in the lower extremity. J. Biomech. 30, 1123–31.

Heintz, S., Gutierrez-Farewik, E.M., 2007. Static optimization of muscle forces during gait in comparison to EMG-to-force processing approach. Gait Posture 26, 279–288.

Inman, V.T., Ralston, H., Todd, F., 1989. Human Walking. Edwin Mellen Pr.

Kadaba, M.P., Ramakrishnan, H.K., Wootten, M.E., Gainey, J., Gorton, G., Cochran, G. V, 1989. Repeatability of kinematic, kinetic, and electromyographic data in normal adult gait. J Orthop Res 7, 849–60.

Kepple, T.M., Sommer 3rd, H.J., Lohmann Siegel, K., Stanhope, S.J., 1998. A three-dimensional musculoskeletal database for the lower extremities. J Biomech 31, 77–80.

Keyak, J.H., Fourkas, M.G., Meagher, J.M., Skinner, H.B., 1993. Validation of an automated method of three-dimensional finite element modelling of bone. J. Biomech. Eng. 15, 505–509.

Kröger, H., Lunt, M., Reeve, J., Dequeker, J., Adams, J.E., Birkenhager, J.C., et al., 1999. Bone density reduction in various measurement sites in men and women with osteoporotic fractures of spine and hip: the European quantitation of osteoporosis study. Calcif Tissue Int 64, 191–9.

Kummer, B., 1993. Is the Pauwels' theory of hip biomechanics still valid? A critical analysis, based on modern methods. Ann. Anat. 175, 203–10.

Leardini, A., Sawacha, Z., Paolini, G., Ingrosso, S., Nativo, R., Benedetti, M.G., 2007. A new anatomically based protocol for gait analysis in children. Gait Posture 26, 560–71.

Li, J., Mashiba, T., Burr, D.B., 2001. Bisphosphonate treatment suppresses not only stochastic remodeling but also the targeted repair of microdamage. Calcif. Tissue Int. 69, 281–6.

Martelli, S., Kersh, M.E., Schache, A.G., Pandy, M.G., 2014. Strain energy in the femoral neck during exercise. J. Biomech. In Press. dx.doi.org/10.1016/j.jbiomech.2014.03.036

Martelli, S., Taddei, F., Cappello, A., van Sint Jan, S., Leardini, A., Viceconti, M., 2011. Effect of sub-optimal neuromotor control on the hip joint load during level walking. J. Biomech. 44, 1716–1721. doi:10.1016/j.jbiomech.2011.03.039

Morgan, E.F., Bayraktar, H.H., Keaveny, T.M., 2003. Trabecular bone modulus-density relationships depend on anatomic site. J. Biomech. 36, 897–904.

Roschger, P., Rinnerthaler, S., Yates, J., Rodan, G.A., Fratzl, P., Klaushofer, K., 2001. Alendronate increases degree and uniformity of mineralization in cancellous bone and decreases the porosity in cortical bone of osteoporotic women. Bone 29, 185–91.

Saita, Y., Ishijma, M., Mogami, A., Gen, H., Kaneko, K., Miyagawa, K., Nemoto, M., et al., 2012. Association between the Fracture Site and the Mechanical Axis of Lower Extremities in Patients with Atypical Femoral Fracture. J. Bone Miner. Res. 27.

Saleh, A., Hegde, V. V, Potty, A.G., Schneider, R., Cornell, C.N., Lane, J.M., 2012. Management strategy for symptomatic bisphosphonate-associated incomplete atypical femoral fractures. HSS J. 8, 103–10. doi:10.1007/s11420-012-9275-y

Sasaki, S., Miyakoshi, N., Hongo, M., Kasukawa, Y., Shimada, Y., 2012. Low-energy diaphyseal femoral fractures associated with bisphosphonate use and severe curved femur: a case series. J. Bone Miner. Metab. 30, 561–7. doi:10.1007/s00774-012-0358-0

Schileo, E., Taddei, F., Malandrino, A., Cristofolini, L., Viceconti, M., 2007. Subject-specific finite element models can accurately predict strain levels in long bones. J. Biomech. 40, 2982–9. doi:10.1016/j.jbiomech.2007.02.010

Shane, E., Burr, D., Abrahamsen, B., Adler, R., Brown, T., Cheung, A., et al., 2013. Atypical Subtrochanteric and Diaphyseal Femoral Fractures: Second Report of a Task Force of the American Society for Bone and Mineral Research. J. Bone Miner. Res. under revi.

Shane, E., Burr, D., Ebeling, P.R., Abrahamsen, B., Adler, R. a, Brown, T.D., Cheung, A.M., et al., 2010. Atypical subtrochanteric and diaphyseal femoral fractures: report of a task force of the American Society for Bone and Mineral Research. J. Bone Miner. Res. 25, 2267–94. doi:10.1002/jbmr.253

Stacoff, A., Diezi, C., Luder, G., Stüssi, E., Kramers-de Quervain, I.A., 2005. Ground reaction forces on stairs: effects of stair inclination and age. Gait Posture 21, 24–38. doi:10.1016/j.gaitpost.2003.11.003

Testi, D., Quadrani, P., Viceconti, M., 2010. PhysiomeSpace: digital library service for biomedical data. Philos. Trans. A. Math. Phys. Eng. Sci. 368, 2853–61. doi:10.1098/rsta.2010.0023

Valente, G., Martelli, S., Taddei, F., Farinella, G., Viceconti, M., 2012. Muscle discretization affects the loading transferred to bones in lowerlimb musculoskeletal models. Proc. Inst. Mech. Eng. Part H J. Eng. Med. 226, 161–9. doi:10.1177/0954411911425863

Vashishth, D., 2009. Advanced glycation end-products and bone fractures. IBMS Bonekey 6, 268–278. doi:10.1138/20090390

Viceconti, M., Clapworthy, G. & Van Sint Jan, S. 2008 The Virtual Physiological Human - a European initiative for in silico human modelling - A European Initiative for in silico Human Modelling. J. Physiol. Sci. 58, 441–6. doi:10.2170/physiolsci.RP009908

Wu, G., Siegler, S., Allard, P., Kirtley, C., Leardini, A., Rosenbaum, D., et al., 2002. ISB recommendation on definitions of joint coordinate system of various joints for the reporting of human joint motion--part I: ankle, hip, and spine. International Society of Biomechanics. J. Biomech. 35, 543–548.

TABLES

Table 1 – Anthropometrical parameters and weight of the participant and the donor

Parameter	Participant (female, 25 years old)	Donor (female, 81 years old)
High (cm)	165	167
Weight (kg)	57	63
Pelvis width (cm)	241	24.4
Femoral length (cm)	44.4	45.2
Shank length (cm)	39.4	42.9

FIGURE CAPTIONS

Figure 1 – The modeling procedure: the body musculoskeletal and the femur finite-element models (a), the motion data (b) and an intermediate frame of simulated stair ascent (c).

Figure 2 – Comparison of the tensile strain pattern during an intermediate frame of walking (left) with typical AFFs onset locations arrowed in an X-ray view (right) courtesy of Saleh et al. (Saleh et al., 2012). The FE map is mirrored to facilitate comparison of the right femur model with the left femur represented in the X-ray.

Figure 3 – Cortical tensile and compressive strain patterns in four transversal section of the femoral shaft at five time intervals during the stance phase of walking.

Figure 4 - Cortical tensile (red) and compressive (blue) strain patterns in four transversal section of the femoral shaft at five time intervals during the stance phase of stair ascent.

Figure 5 – Average tensile (red) and compressive (blue) strain levels during the stance phase of each studied activity along the frontal, posterior, medial and lateral femoral shaft.

Figure 6 – Linear regression analysis between tensile strains in the lateral femoral shaft and the hip adduction moment during the six studied activities.

Figure 1

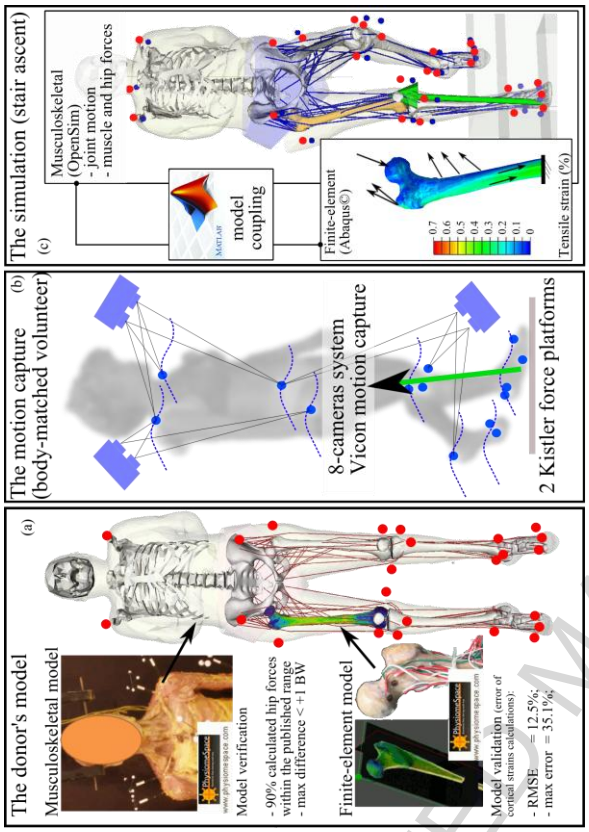

Figure 2

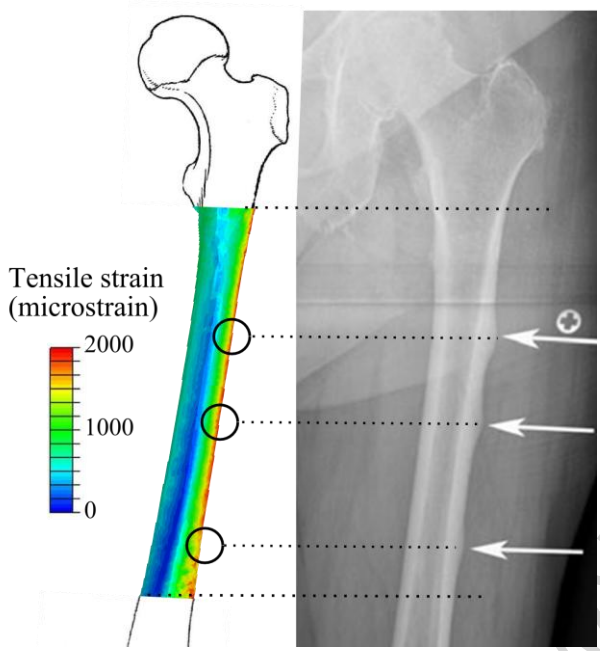

Figure 3

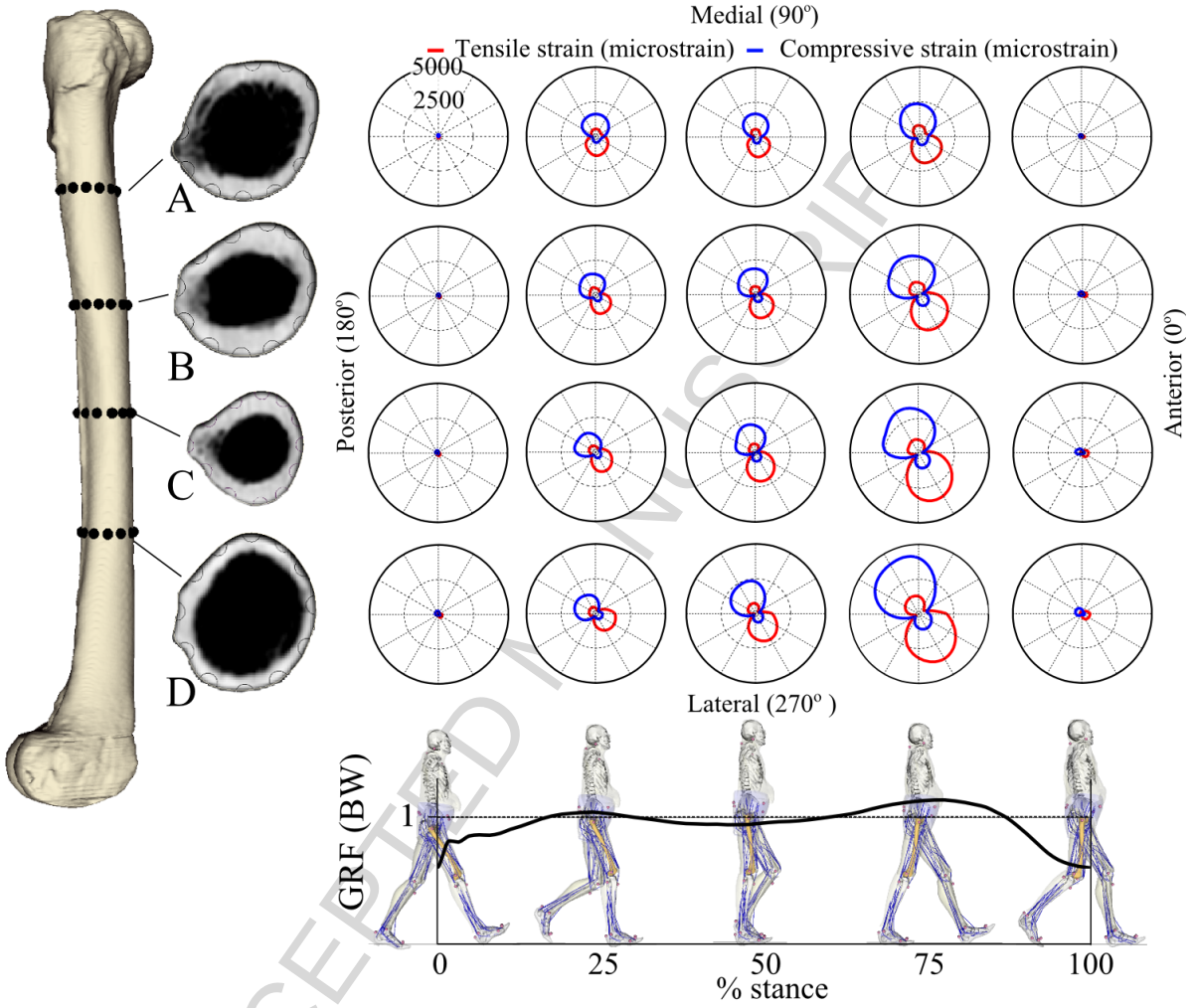

Figure 4

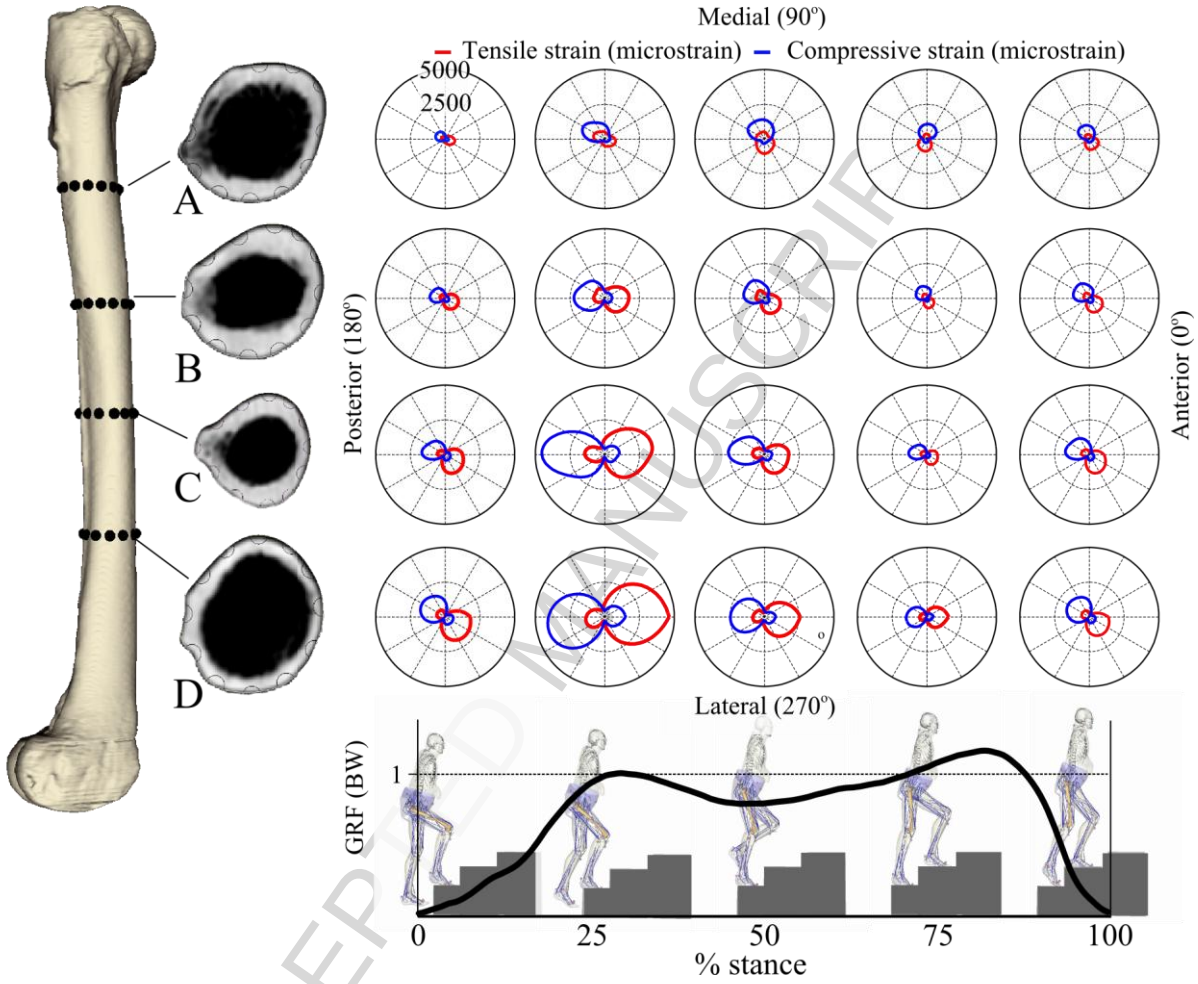

Figure 5

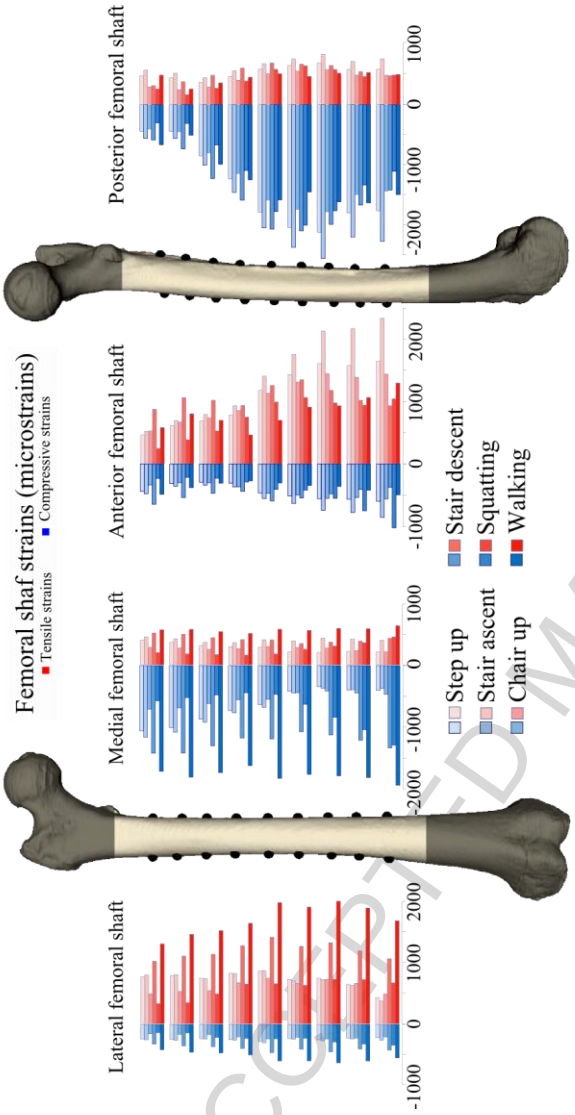

Figure 6

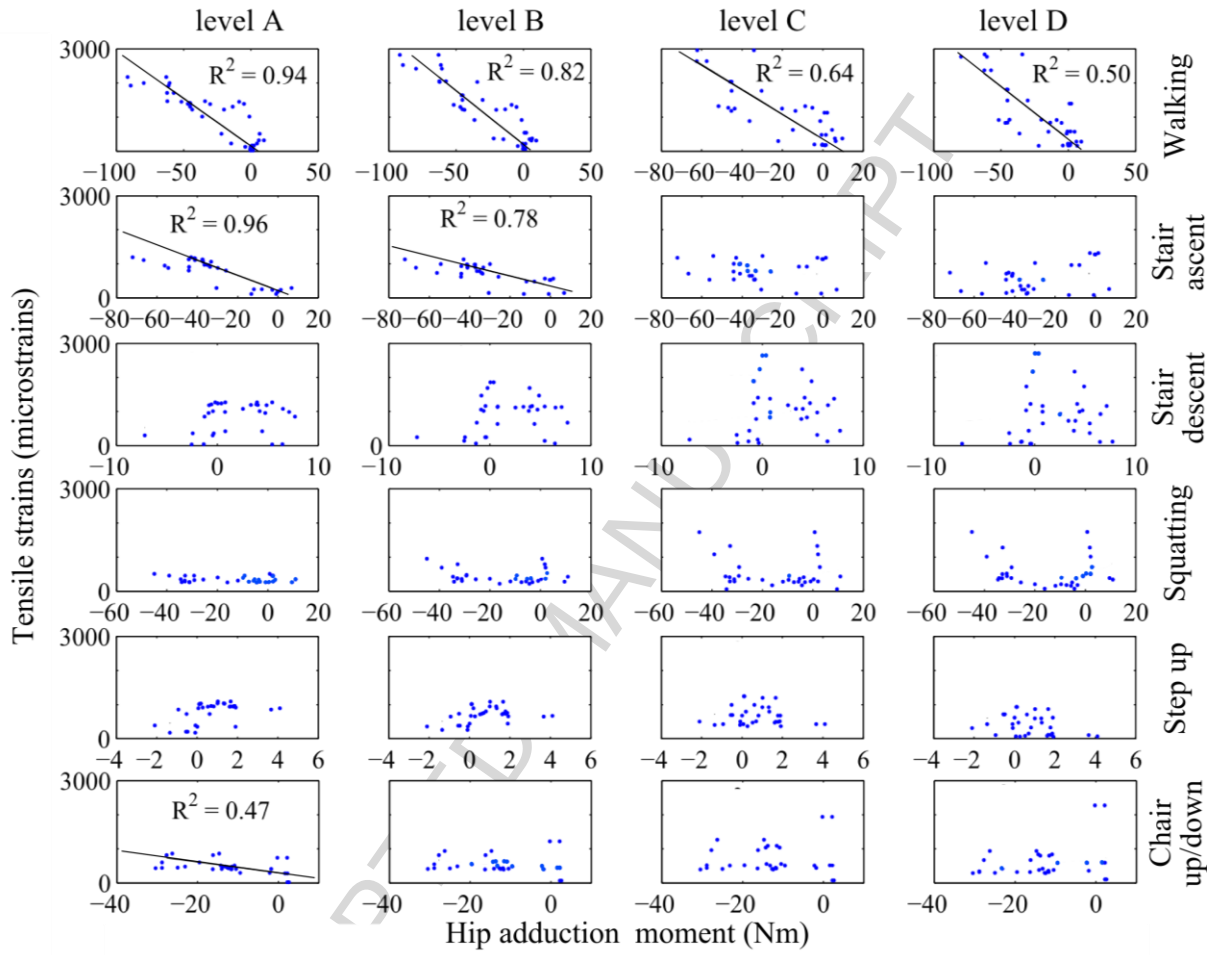

SUPPLEMENTARY MATERIAL

Supplemental figure 1 – The ground reaction forces at the right foot recorded during the selected trial of the six studied activities (solid black line). Grey bands represent the available normality patterns (Bergmann et al., 2001; Stacoff et al., 2005)

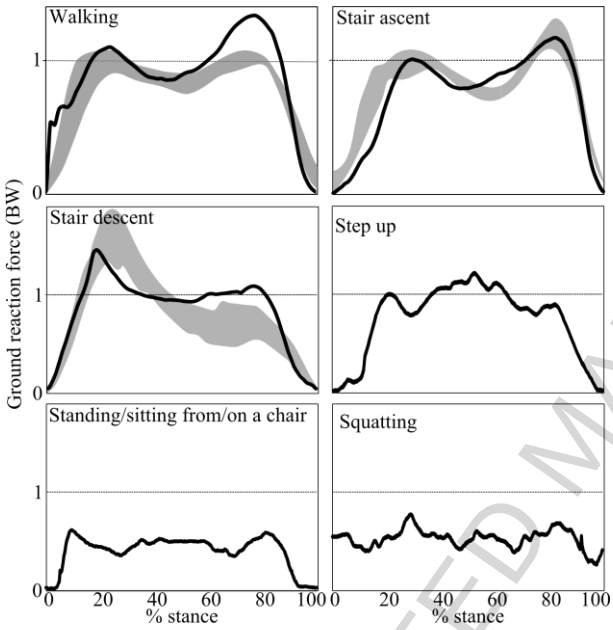

Supplemental figure 2 – Comparison of the calculated joint kinematics (a) and joint net moments (b) with the corresponding normality patterns reported by Kadaba et al. (1989) and comparison of the calculated active phase for the principal lower-limb muscles (solid red) with expected phases of muscles electrical activity reported by Inman et al. (1989).

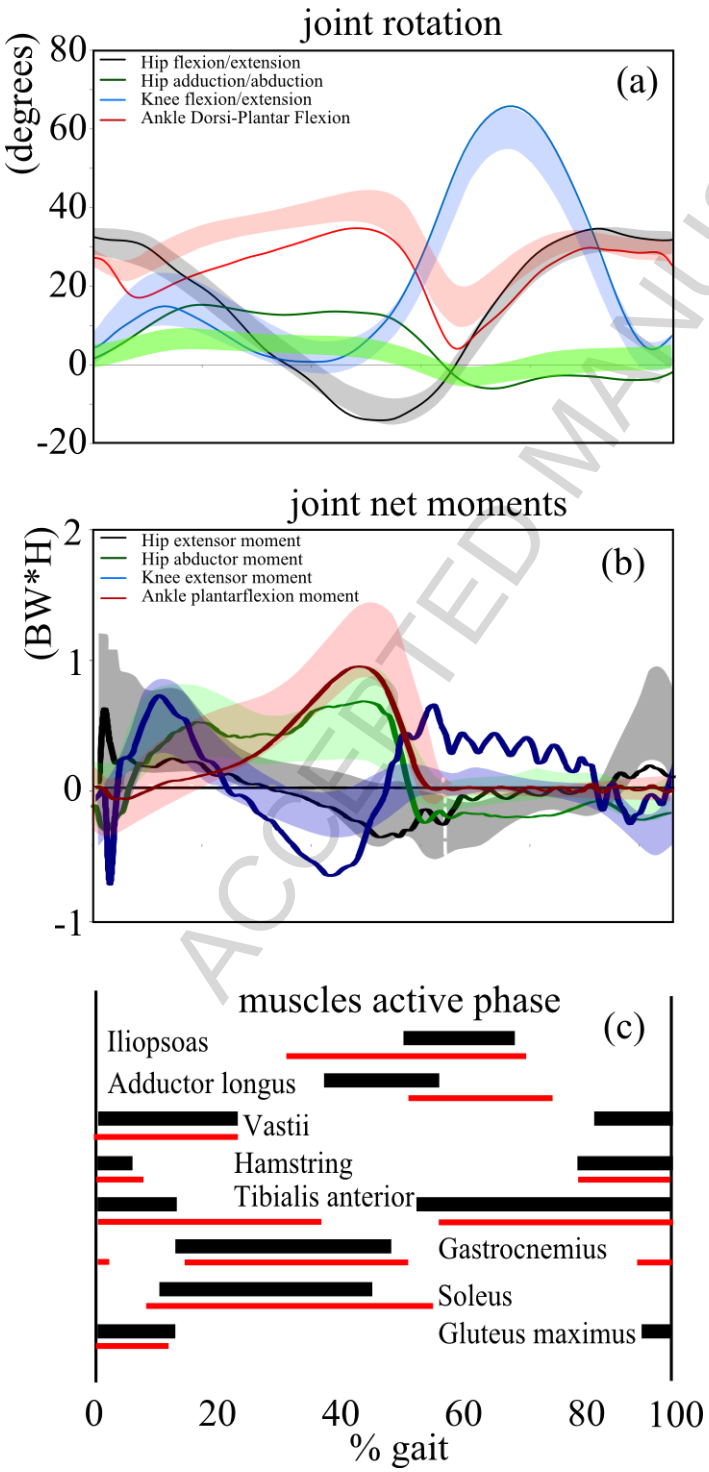

Supplemental figure 3 –Calculated hip forces (red dots) and the envelope (blue band) of published hip force measurements (Bergmann et al., 2011; www.orthoload.com). Forces are expressed in body-weight (BW).

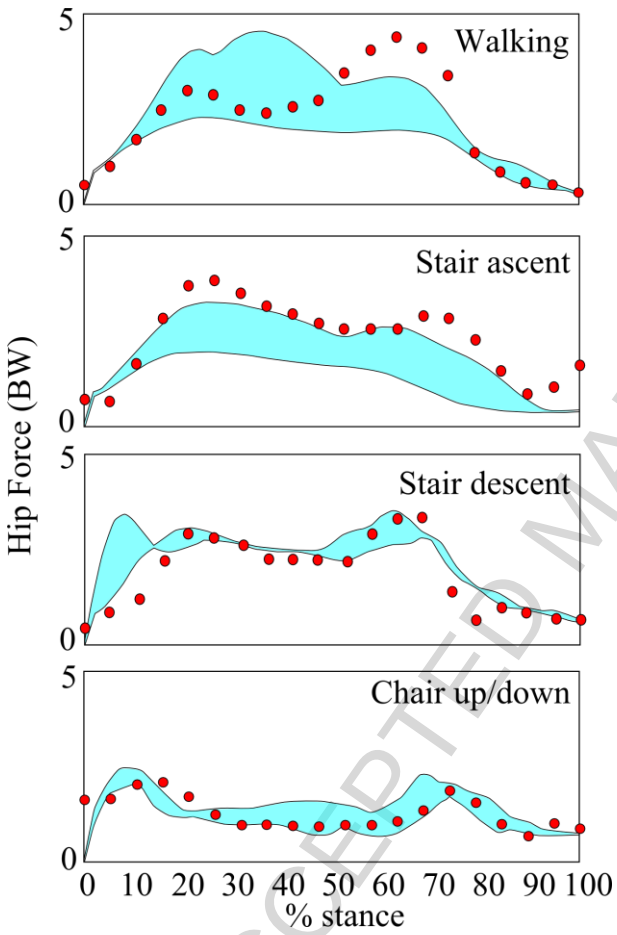

Supplemental Figure 8 – Free body diagram of the femur representing the muscle force orientations (black arrows), muscle attachment points (red dots), the femoral coordinate system calculated according to the ISB standards (Wu et al., 2002) and the anatomical landmarks (femur epicondyles and center of the femoral head) used to calculate the femoral coordinate system (blue dots).

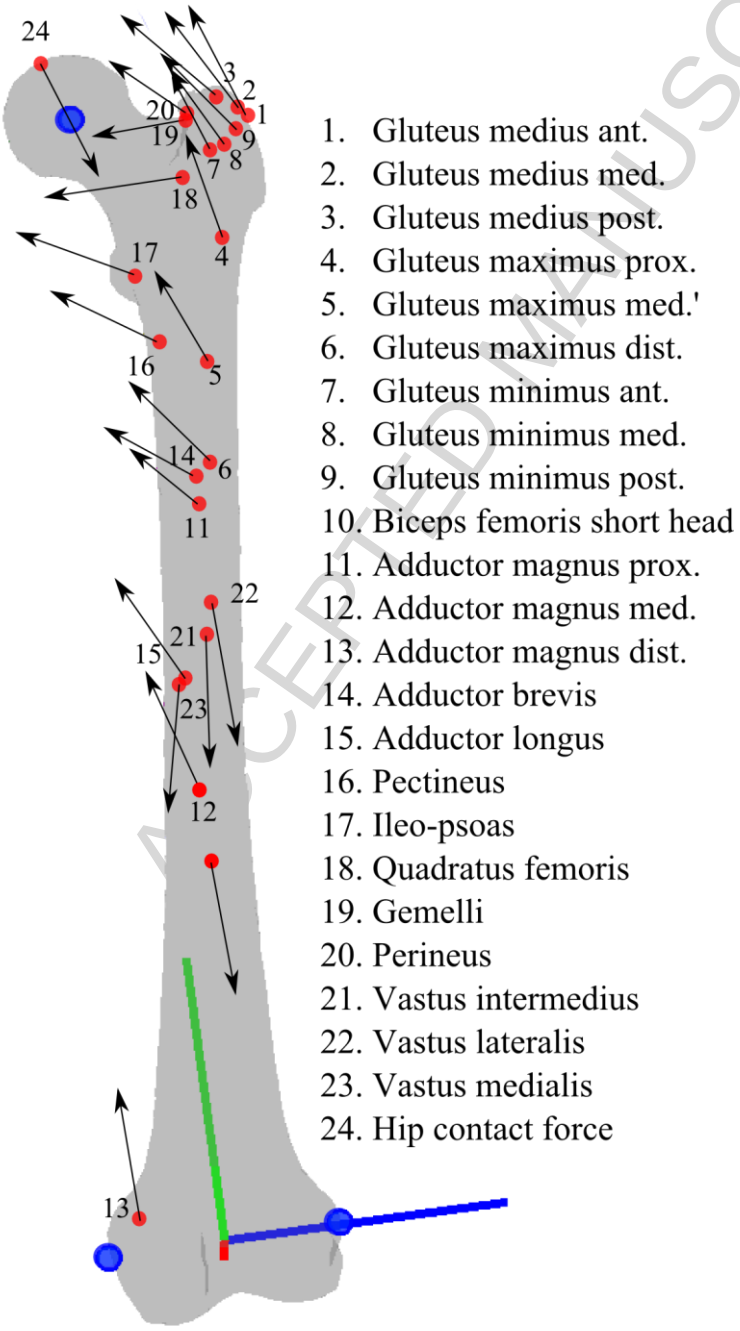

1. Gluteus medius ant.
2. Gluteus medius med.
3. Gluteus medius post.
4. Gluteus maximus prox.
5. Gluteus maximus med.'
6. Gluteus maximus dist.
7. Gluteus minimus ant.
8. Gluteus minimus med.
9. Gluteus minimus post.
10. Biceps femoris short head
11. Adductor magnus prox.
12. Adductor magnus med.
13. Adductor magnus dist.
14. Adductor brevis
15. Adductor longus
16. Pectineus
17. Ileo-psoas
18. Quadratus femoris
19. Gemelli
20. Perineus
21. Vastus intermedius
22. Vastus lateralis
23. Vastus medialis
24. Hip contact force

Supplemental Figure 4 - Cortical tensile (red) and compressive (blue) strain patterns in four transversal section of the femoral shaft at five time intervals during the stance phase of stair descent.

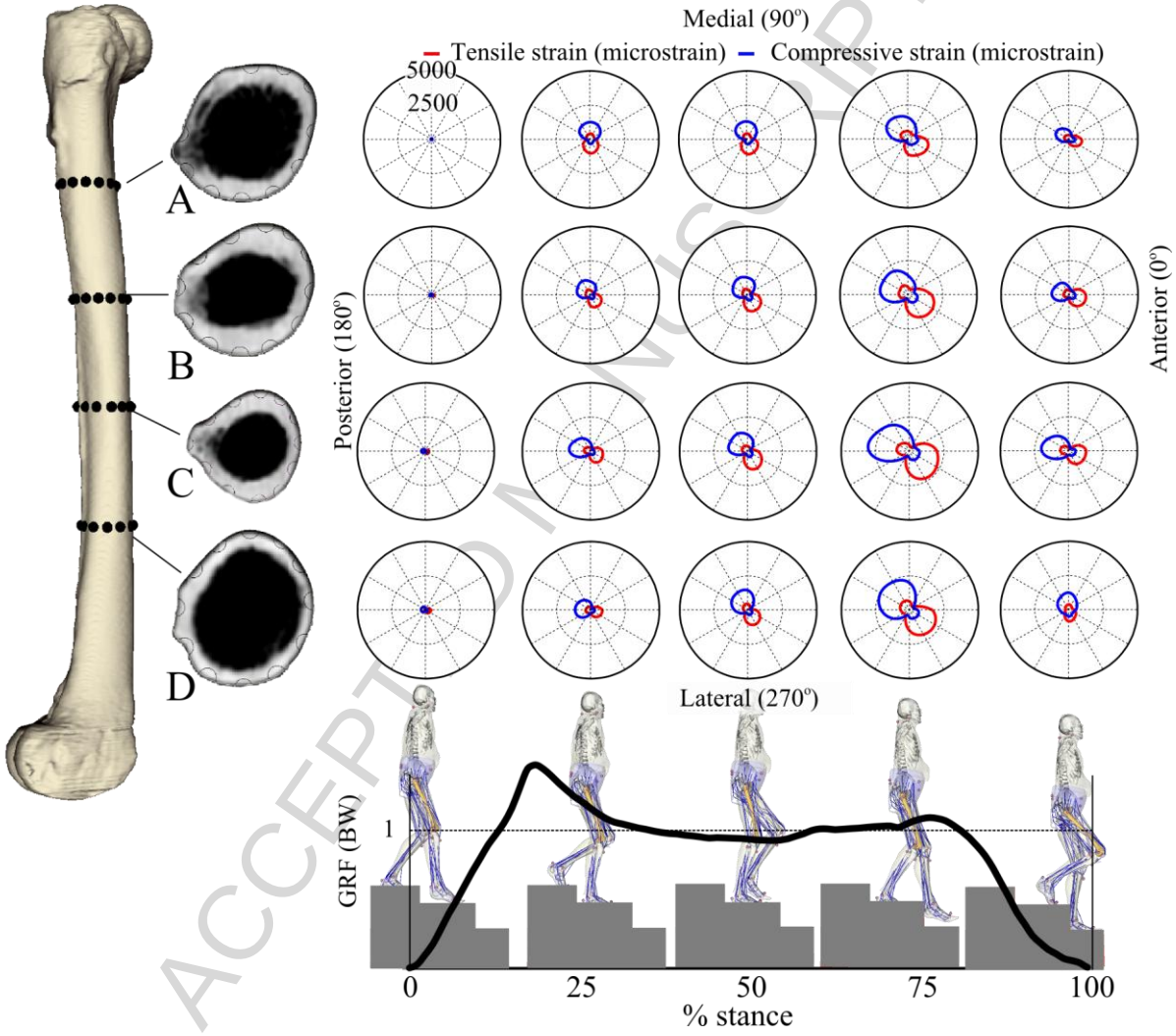

Supplemental Figure 5 - Cortical tensile (red) and compressive (blue) strain patterns in four transversal section of the femoral shaft at five time intervals during rising from and sitting on a chair.

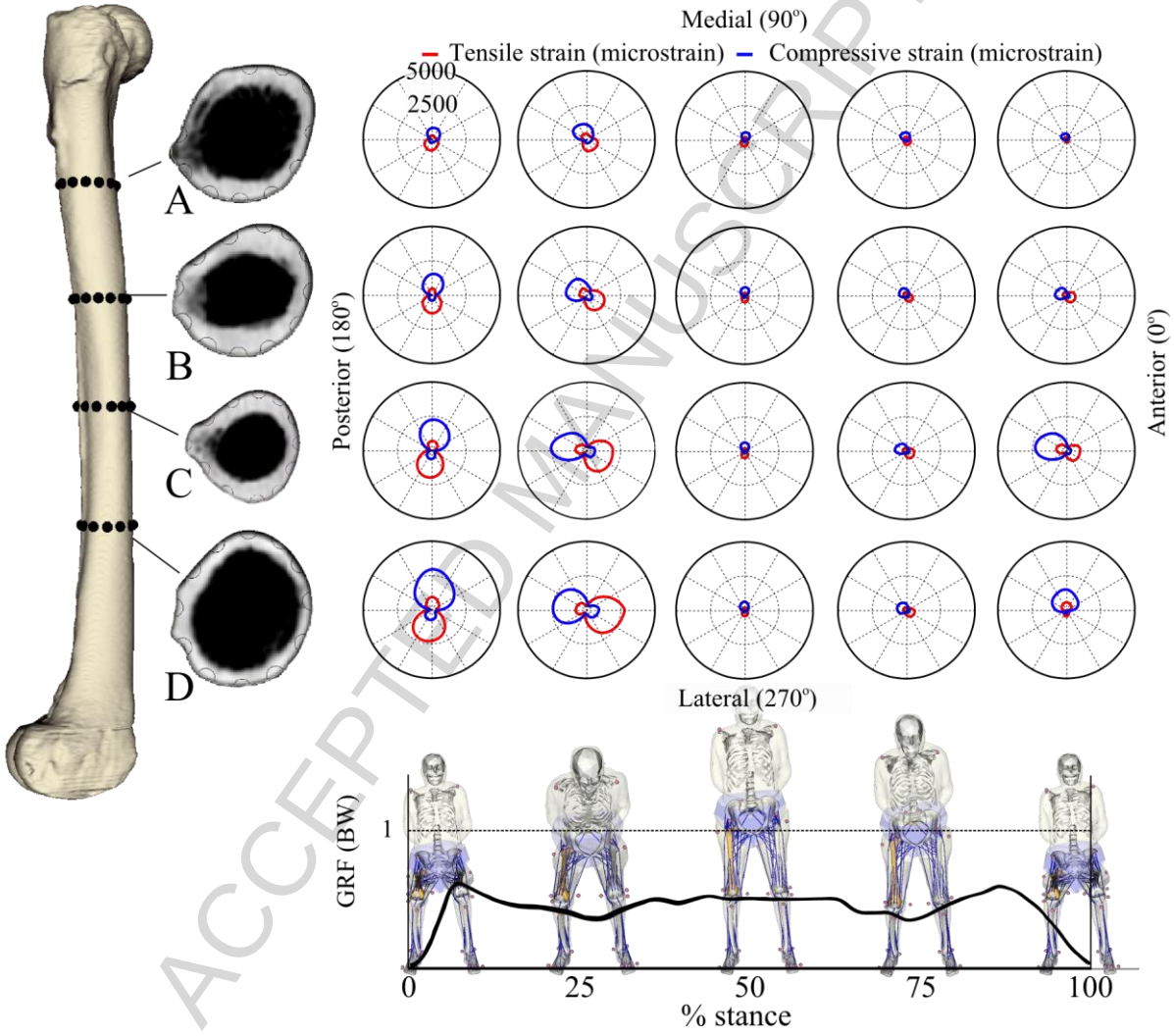

Supplemental Figure 6 - Cortical tensile (red) and compressive (blue) strain patterns in four transversal section of the femoral shaft at five time intervals during step up.

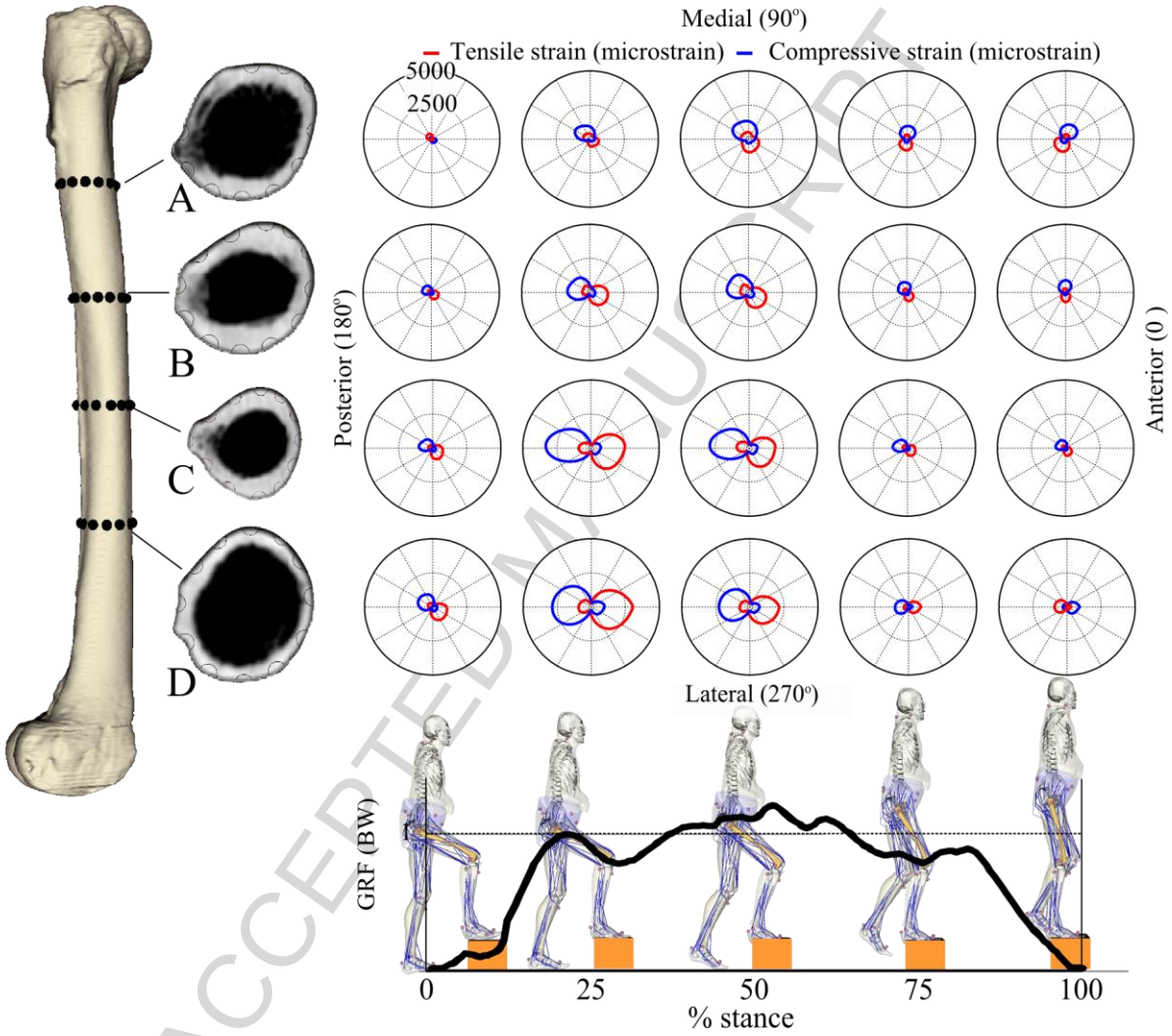

Supplemental Figure 7 - Cortical tensile (red) and compressive (blue) strain patterns in four transversal section of the femoral shaft at five time intervals during squatting.

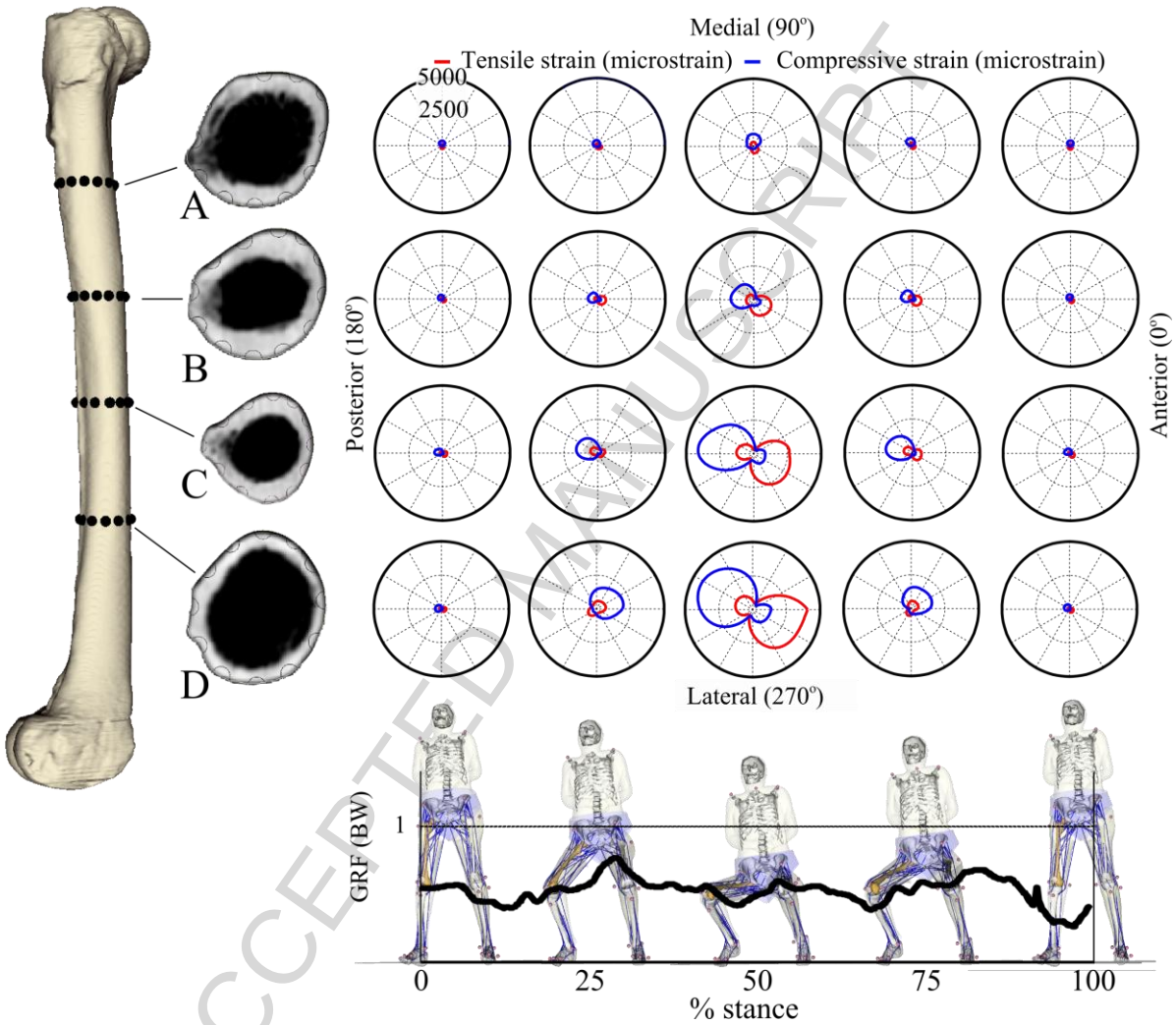

HIGHLIGHTS

- Atypical femoral fracture onset may be associated with daily femoral strain patterns.
- We modelled bone strains in the femoral shaft during daily activities.
- We found that the lateral femoral shaft is loaded in tension up to activity-dependent levels.
- Atypical femoral fractures are associated with daily tensile loads.
- Walking causes the highest tensile strains in the lateral shaft among daily activities.